Available online at www.sciencedirect.com

SciVerse ScienceDirect

journal homepage: www.elsevier.com/locate/he

Enhanced performance of LSCF cathode through surface modification

Mingfei Liu [b], *Dong Ding* [b], *Kevin Blinn* [b], *Xiaxi Li* [b], *Lifang Nie* [b], *Meilin Liu* [a,*]

[a] *World Class University (WCU) Program, UNIST, South Korea*

[b] *Center for Innovative Fuel Cell and Battery Technologies, School of Materials Science and Engineering, Georgia Institute of Technology, 771 Ferst Drive, N.W., Atlanta, GA 30332, USA*

ARTICLE INFO

Article history:
Received 1 February 2012
Received in revised form
23 February 2012
Accepted 24 February 2012
Available online 24 March 2012

Keywords:
SOFC
LSCF cathode
LCC catalyst coating
Surface enhancement
Stability

ABSTRACT

Mixed ionic-electronic conductors in the family of $La_xSr_{1-x}Co_yFe_{1-y}O_{3-\delta}$ (LSCF) have been widely studied as cathode materials for solid oxide fuel cells (SOFCs). However, the long-term stability and the limited surface catalytic activity are still a concern. Here we report a new catalyst $La_{0.4875}Ca_{0.0125}Ce_{0.5}O_{2-\delta}$ (LCC), which can significantly enhance the performance and stability of LSCF cathodes when applied as a thin-film coating on LSCF surface. For example, with 5 μL 0.25 mol L^{-1} LCC solution infiltrated into LSCF cathode, the cathodic polarization resistance was reduced by ~60% (to ~0.076 Ω cm^2) at 750 °C, leading to a peak power density of ~1.25 W/cm^2, which is ~18% higher than that for the unmodified LSCF cathode in an anode-supported cell. In addition, stable power output was observed for over 500 h operation at 750 °C under a constant voltage of 0.7 V.

1. Introduction

In recent years, the $La_xSr_{1-x}Co_yFe_{1-y}O_{3-\delta}$ (LSCF) based cathode for SOFCs has been extensively investigated due to its much higher ionic and electronic conductivity and hence better performance than the conventional LSM cathode [1–3] in the temperature range of 600–800 °C. However, the long-term stability of LSCF cathodes is a concern for practical applications [4–6]. Additionally, the oxygen reduction reaction on LSCF cathode is likely limited by the surface exchange process rather than the bulk charge transport process [7–9].

In order to enhance the performance and/or stability of LSCF cathode, several approaches have been studied, including using composite cathode of LSCF-SDC [10,11], LSCF-GDC [2], LSCF-Ag [12] and LSCF-SDC-Ag [13], or using precious metal such as Pt, Pd, and Ag [14–16] to coat the LSCF surface and enhance its performance. Recently, we proposed a method to improve the performance and stability of a porous LSCF cathode by application of a thin catalytically active coating through infiltration [17]. Improved performance and stability have been demonstrated using thin coating of LSM [9], SSC [18] and SDC [19] on LSCF. Compared to the aforementioned work [2,10–16], this approach can be more readily incorporated in the current fabrication processes at low cost.

Here we report a new catalyst, $La_{0.4875}Ca_{0.0125}Ce_{0.5}O_{2-\delta}$ (LCC), for LSCF cathode surface modification. Doped ceria compounds have been widely used as catalyst materials due to their high ionic conductivity, favorable surface exchange properties, and oxygen storage capability [20]. Among various dopants studied, La incorporated into the cerium site can significantly enhance the oxygen transfer capability [21]. Although LCC displays relatively poor ionic conductivity,

* *Corresponding author*. Tel.: +1 404 894 6114; fax: +1 404 894 9140.
E-mail addresses: mingfei.liu@mse.gatech.edu (M. Liu), meilin.liu@mse.gatech.edu (M. Liu).

0360-3199/$ – see front matter Copyright © 2012, Hydrogen Energy Publications, LLC. Published by Elsevier Ltd. All rights reserved.
doi:10.1016/j.ijhydene.2012.02.139

the high doping level of ceria by La and Ca (i.e. 50% mol. total substitution) creates high surface oxygen vacancy concentration. When the LSCF cathode is modified by a thin LCC coating, the surface layer with high oxygen vacancy concentration may enhance oxygen molecule dissociation into atomic oxygen [22] and facilitate the oxygen reduction reaction. Even more importantly, the LCC coating can alleviate the enrichment of Sr at the LSCF/SDC interface and LSCF grain surface that is believed to be at least partially responsible for the LSCF degradation [4]. The doped ceria shows excellent solubility of SrO [23], which can reduce the driving force of diffusion of Sr from the LSCF cathode to the YSZ electrolyte and thus help prevent the enrichment of Sr on LSCF grain surface that would otherwise block active sites for oxygen reduction. In this manner, LCC coated LSCF may potentially enhance the stability during operation which would ultimately reduce the cost of SOFC technology.

2. Experimental

To evaluate the polarization resistance of the modified LSCF cathodes, we used symmetric cells with two identical LSCF cathodes on both sides of the YSZ electrolyte: LSCF|SDC|YSZ|SDC|LSCF. Further, the performance enhancement was also validated in anode-supported button cells with a configuration of Ni-YSZ|YSZ|SDC|LSCF.

YSZ electrolyte was used for construction of symmetrical cells in this study so that the LSCF cathodes for symmetrical cells were identical to those for anode-supported YSZ cell. Cylindrical YSZ pellets were prepared by uniaxially pressing a commercially available YSZ powder (Daiichi Kigenso, Japan) followed by sintering at 1450 °C for 5 h to achieve relative density of ~98%. LSCF (from Fuel Cell Materials) green tapes prepared by tape-casting [24] (~50 μm) were then bound onto both sides of a YSZ pellet using a slurry of $Sm_{0.2}Ce_{0.8}O_{2-\delta}$ (SDC, 3–4 μm) as a buffer layer, which was subsequently co-fired with SDC on YSZ at 1080 °C for 2 h to form porous LSCF electrodes with an active area of 0.3 cm^2. The SDC powder was synthesized using a chemical co-precipitation process [25,26]. The SDC powder was then dispersed in acetone with V-006 as binder and ball-milled for 24 h to form a stable SDC slurry.

Aqueous nitrate solutions of LCC precursors with different concentrations (0.05, 0.10, 0.125, 0.25 and 0.5 mol L^{-1}) were prepared by dissolving proper amounts of $La(NO_3)_3 \cdot 6H_2O$, $Ca(NO_3)_2 \cdot 4H_2O$, $Ce(NO_3)_3 \cdot 6H_2O$ and glycine in distilled water. Glycine was used as a complexing agent to facilitate the phase formation. For each surface modification, 5 μL of LCC solution was infiltrated into a porous LSCF electrode using a micro-liter syringe to control the amount of loading. The infiltrated cell was then fired at 900 °C in air for 1 h to obtain the LCC-infiltrated LSCF. The ASR of cathodes was measured in a two-electrode symmetric cell configuration using two Pt meshes as current collector (without Pt paste to avoid the possible catalytic contribution from Pt). Impedance spectra were acquired using a Solartron 1255 HF frequency response analyzer interfaced with an EG&G PAR potentiostat model 273A with an amplitude of 10 mV in the frequency range from 100 kHz to 0.1 Hz.

For comparison, a mixture of LSCF and LCC with weight ratio of 7:3 was mixed thoroughly with V-006 binder to prepare cathode slurry, and the slurry was then applied to both sides of sintered SDC pellets by brush-painting followed by sintering at 1050 °C to assemble a symmetrical cell. Pure LSCF cathodes and LSCF-SDC (weight ratio of 7:3) composite cathodes were also prepared using the same method for comparison.

To fabricate anode-supported button cells, a tape-cast NiO-YSZ anode-support was first fabricated and pre-fired at 900 °C for 2 h. Then, an active NiO-YSZ layer (~15 μm) and YSZ electrolyte (~15 μm) were sequentially deposited on the anode support by a particle suspension coating process [27,28] followed by co-firing at 1400 °C for 5 h. The LSCF cathode was then applied to the YSZ electrolyte using the same procedures for the fabrication of symmetric cells as described earlier. 5 μL 0.25 mol L^{-1} LCC solution was infiltrated into cathode followed by firing at 900 °C for 1 h. The whole cell was mounted and sealed on a fuel cell testing fixture, and then tested with humidified hydrogen (3 %H_2O) as fuel and ambient air as oxidant. The cell performances were examined with an Arbin multi-channel electrochemical testing system (MSTAT).

X-ray diffraction (XRD) analysis was used to examine the phase purity of the LCC powders (derived from nitrate solutions) and the LSCF powder as well as the chemical compatibility between LCC and LSCF. The microstructure and morphology of the LCC-infiltrated LSCF cathode was examined using a thermally assisted field emission scanning electron microscope (SEM, LEO 1530). Raman spectroscopy (Renishaw RM 1000, 514 nm excitation) was also performed on both LCC-infiltrated and unmodified cathodes before and after long-term operation of the full cells.

3. Results and discussion

3.1. Structural characterization

Shown in Fig. 1 are the XRD patterns of LCC powders derived from the infiltration solution and subsequently fired at different temperatures. A fluorite phase of LCC, with

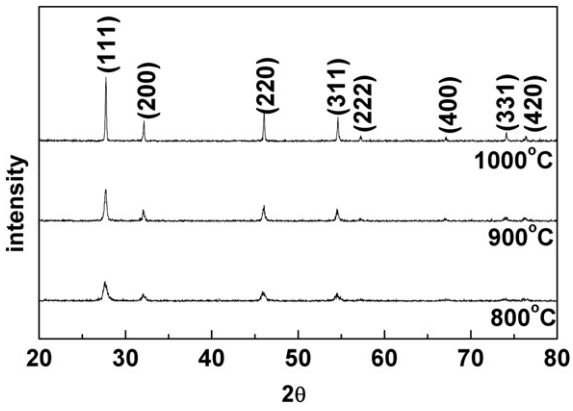

Fig. 1 – X-ray diffraction patterns of LCC powders derived from the infiltration solution and subsequently fired at different temperatures.

$a = 5.5680(1)$ Å, was formed at 800 °C. The main peaks became sharper at higher temperatures, indicating some grain growth. The grain sizes calculated from the Scherrer formula were 10, 20, and 47 nm at firing temperatures of 800, 900, and 1000 °C, respectively. Although finer particles are preferable for initial catalytic activity, grain growth during operation can lower the stability of the fuel cell [29]. For the best overall performance of a fuel cell cathode operated at 750 °C, we used 900 °C as the initial firing temperature for LCC modification of LSCF.

While the purpose of using a thin LCC coating on LSCF is to enhance the surface catalytic properties of LSCF, the chemically compatibility of the two phases is very important to the performance and stability of the cathode. The chemical compatibility of LCC with LSCF was investigated by calcining the mixture of LCC and LSCF powders (weight ratio of 1:1) at high temperatures. Shown in Fig. 2 are the XRD patterns of the LCC-LSCF mixture after calcination at 1000 and 1100 °C for 10 h. No extra peaks or obvious peak shifts were observed, indicating that there were no apparent chemical reactions between LSCF and LCC even when they were fired at 1100 °C, suggesting that the LCC and LSCF have a good chemical compatibility even at high temperatures.

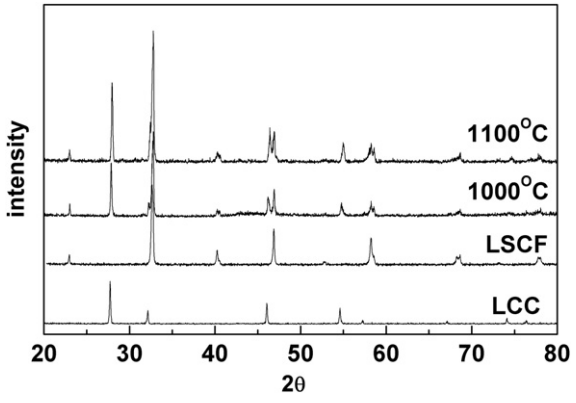

Fig. 2 – XRD pattern of LCC and LSCF fired at different temperatures for 10 h.

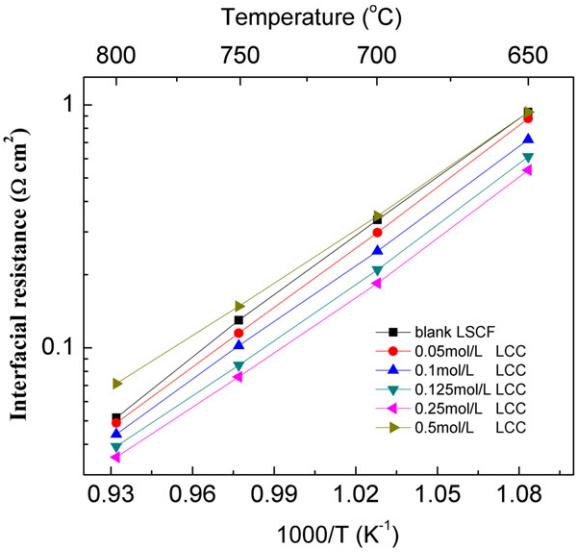

Fig. 3 – Interfacial polarization resistances of porous LSCF electrodes, without or with infiltration of 5 μL different concentrations of LCC solution, as determined from impedance spectra acquired from symmetrical cells tested in air at different temperatures.

3.2. *Electrochemical activity*

Fig. 3 summarizes the effect of LCC infiltration on electrode polarization resistances (Rp, determined from the impedance spectra) at 650–800 °C under open circuit conditions. As can be seen in Fig. 3, the blank LSCF cell exhibited an area specific resistance of 0.130 Ω cm^2 at 750 °C, close to the reported value of ~0.12 Ω cm^2 at 750 °C [2]. When infiltrated with the proper amount of LCC coating on LSCF backbone, Rp decreased significantly as the LCC concentration was increased from 0.05 to 0.25 mol L^{-1}. At 750 °C, for example, the Rp was reduced to 0.115, 0.102, 0.085, and 0.076 Ω cm^2 for the 0.05, 0.1, 0.125, and 0.25 mol L^{-1} LCC-infiltrated LSCF, respectively. Among the concentrations of LCC solutions studied, 0.25 mol L^{-1} offered the lowest resistance. When infiltrated with 5 μL 0.25 mol L^{-1} LCC solution, the Rp values were 0.035, 0.076, 0.184, and 0.539 Ω cm^2 at 800, 750, 700, and 650 °C, respectively. However, further increasing the concentration to 0.5 mol L^{-1} resulted in significant reduction of the performance and the Rp was increased to 0.148 Ω cm^2, even higher than that of the LSCF cathode before infiltration. The influence of the LCC concentration on the performance of the LSCF cathode might be explained by the detailed morphologies of the LCC coating on LSCF backbone shown in Fig. 4a–f. Before the infiltration, the blank LSCF cathode showed a uniform, porous and well-sintered structure. The LSCF grain size was in the range of 0.2–0.5 um and the surface of the LSCF grains were clean and smooth (Fig. 4). In contrast, after infiltrating the LSCF with 0.05 mol L^{-1} L LCC solution, a small amount of nanoscale discrete LCC particles were uniformly deposited on the LSCF grain surface and the particle size was in the range of 10–20 nm (Fig. 4b). The nano-particles on LSCF surface significantly increased the number of active sites on LSCF surface, leading to a lower polarization resistance. By further increasing the concentration of LCC solution from 0.05 to 0.25 mol L^{-1}, more LCC nano-particles were formed on LSCF surface, which further increased the number of active sites and reduced the polarization resistance. The improved performance of the LCC-infiltrated LSCF compared to the pure LSCF suggested that the LCC is an effective catalyst for oxygen reduction reaction. However, a higher concentration of LCC, such as 0.5 mol L^{-1}, resulted in larger clusters and thick coating of LCC on LSCF surface (shown in Fig. 4f), which reduced the number of active sites and hence resulted in poor performance. In addition, the low conductivity of LCC (to be discussed later) may block ionic and electronic transport across the LCC coating.

Fig. 5 shows some typical impedance spectra of symmetrical cells with blank or LCC-infiltrated LSCF cathode measured at 750 °C in air under open circuit conditions (OCV). Clearly, LCC infiltration dramatically reduced the interfacial

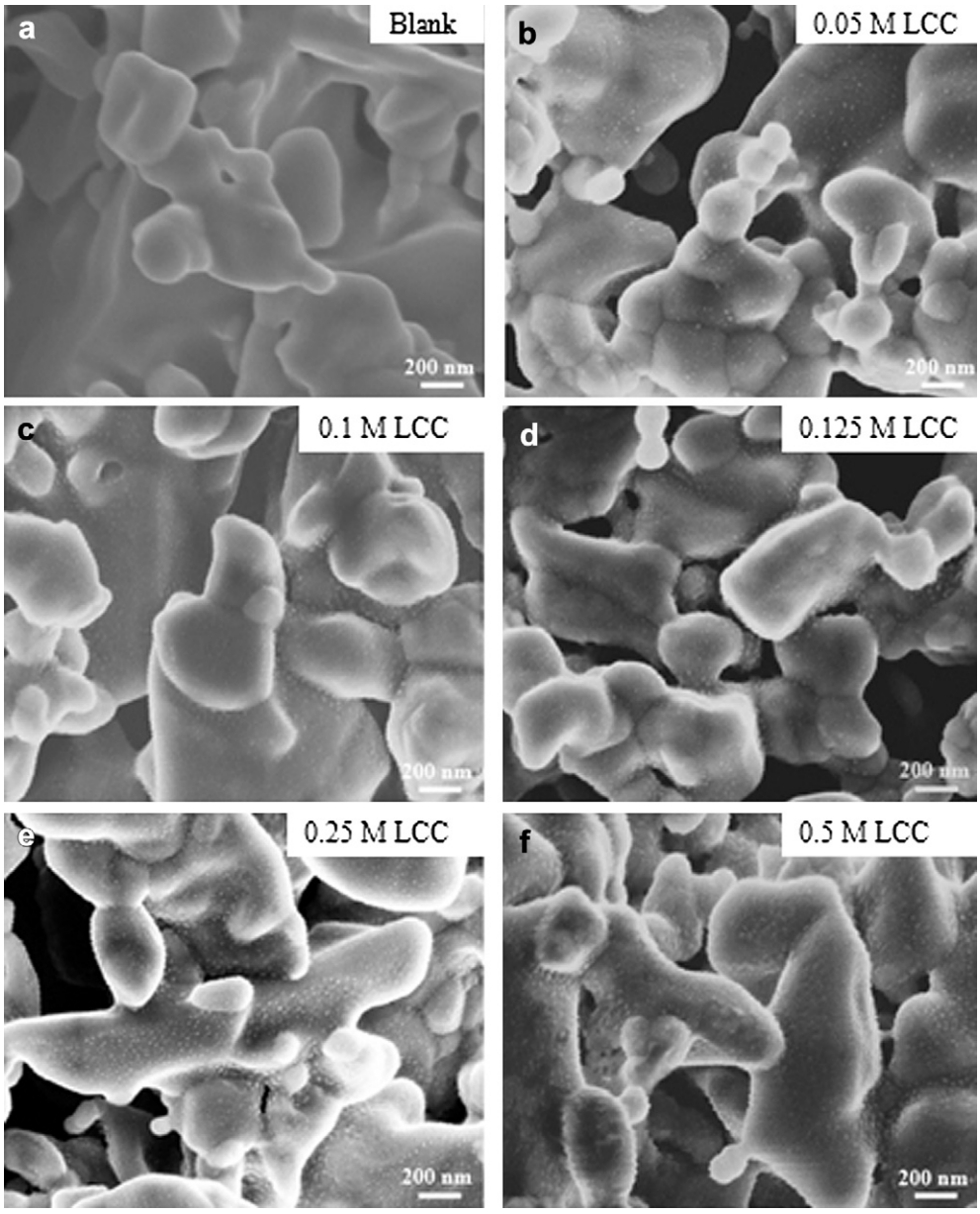

Fig. 4 – Typical surface morphology (SEM images) of (a) a porous LSCF cathode without LCC infiltration and (b)–(f) porous LSCF cathodes infiltrated with 5 μL of LCC solution of different concentrations: (b) 0.05 M, (c) 0.1 M, (d) 0.125 M, (e) 0.25 M and (f) 0.5 M

polarization resistance compared with LSCF cathodes. It appears that all spectra display two separable depressed arcs, implying that at least two different electrode processes make significant contributions to the impedance associated with oxygen reduction reaction. To better understand the effect of LCC infiltration, an equivalent circuit of $LR_0(Q_HR_H)(Q_LR_L)$ was used to fit the impedance data, where L is the inductance arising from the testing fixture, R_0 is the ohmic resistance of the electrolyte and lead wires, (Q_HR_H) corresponds to the high frequency arc, and (Q_LR_L) corresponds to the low frequency arc. Compared with that of the blank LSCF cathode, the impedance loop appearing at low frequencies varied more dramatically with the infiltration of LCC. For example, R_L varied from 0.112 Ω cm^2 for blank LSCF cathode to 0.06 Ω cm^2 for LCC-infiltrated LSCF cathode while R_H just decreased slightly. According to the model electrode analysis of LSCF cathode reported by Maier et al. [30] and Liu et al. [8], the high frequency feature can be assigned to the charge transfer across the interface between the cathode and the electrolyte, while the low frequency feature can be assigned to the electrochemical oxygen surface exchange reaction. The significant reduction of R_L after LCC infiltration indicates that the surface reaction of oxygen species on the LSCF cathode was highly accelerated by the thin LCC coating. However, due to low loading, the LCC has only small effect on the enhancement of charge transfer at the interface.

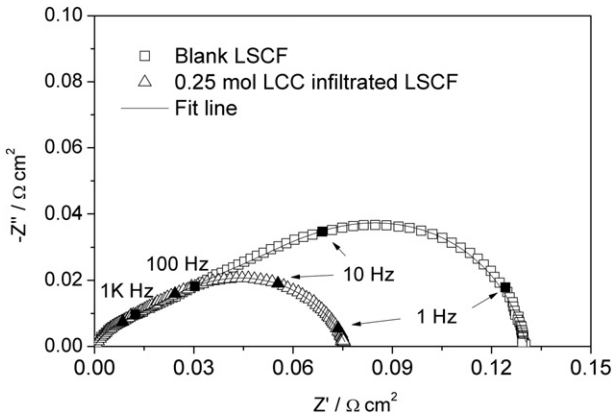

Fig. 5 – Impedance spectra of the blank LSCF and LCC infiltrated (0.25 mol L^{-1}) LSCF at 750 °C.

3.3. *Cell performance in anode-supported cell*

Based on the positive results demonstrated in symmetrical cells, 5uL of 0.25 mol L^{-1} LCC solution was infiltrated into the state-of-the-art anode-supported cell with porous LSCF cathode to investigate the performance and stability upon introduction of LCC coating.

Fig. 6 shows the current–voltage characteristics and the corresponding power density at 750 °C for the anode-supported cells using blank LSCF or LCC-infiltrated LSCF cathodes before and after long-term operation (about 550 h). When humidified hydrogen was used as the fuel and ambient air as the oxidant, a cell with a blank LSCF cathode (without LCC infiltration) yielded a initial peak power density of 1.08 W cm^{-2}, which is comparable to the highest values reported for Ni-YSZ supported SOFCs with LSCF cathodes [31,32]. It should be noted that similar performances were collected from three identical cells, demonstrating good reproducibility of our cell fabrication procedure. The high cell performance provided us a good baseline for the LCC infiltration study; a baseline with poor performance may misguide the study or lead to erroneous conclusions. The cell with LCC infiltration displayed an initial peak power density of ~1.27 W cm^{-2} (Fig. 6), implying 18% improvement in performance.

To study the stability, both cells were run at a constant cell voltage of 0.7 V at 750 °C for about 550 h while the current density was recorded as a function of time, as shown in Fig. 7. Clearly, some degradation was observed for the blank LSCF cathode, as the current density dropped from 1.18 A cm^{-2} to 1.04 A cm^{-2}. The degradation rate was ~12% over 500 h (~0.02% per hour), which is lower than the values reported in the literature (0.06–0.17% per hour) for anode-supported YSZ cells with LSCF cathodes operated under similar conditions [4,5]. For the cells with LCC-infiltrated LSCF cathodes, in contrast, the current density increased slightly in the first few hours and became stabilized thereafter until the end of the test. After 550 h of testing, the current density of the cell with LCC modification was ~0.4 A cm^{-2} higher than that of the cell without LCC modification, demonstrating ~40% performance enhancement. The cell performance measured after the durability test is also presented in Fig. 6. An increase in power output was observed for the LCC-infiltrated cell while the performance of the blank cell underwent a significant decrease after durability test. The corresponding peak power densities were about 1.29 and 0. 95 W cm^{-2}, suggesting that both power density and stability can be enhanced through LCC infiltration.

Shown in Fig. 8 are some typical Raman spectra collected from LSCF cathodes with or without LCC modification before and after the 550 h operation. A typical Raman spectrum from the LSCF cathode before operation consisted mainly of two broad peaks centered at 546 cm^{-1} and 632 cm^{-1}, which correspond to E_g modes characteristic to the structure of $R\bar{3}c$ [33], which is the space group of LSCF [34]. When Raman analysis was performed on the LSCF cathode following long-term operation, the intensities of the two E_g peaks decreased considerably while two new sharp peaks appeared at 675 cm^{-1} and 995 cm^{-1}. These changes were indicative of the

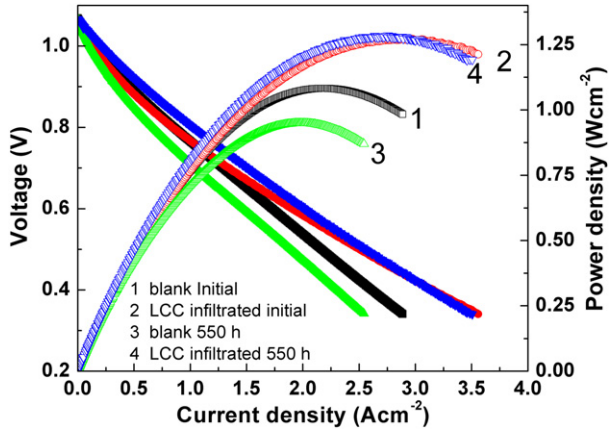

Fig. 6 – Some typical performance of anode-supported button cells, without or with the LSCF cathode infiltrated with 5 μL 0.25 M LCC solution, as measured using humidified hydrogen as fuel and air as oxidant.

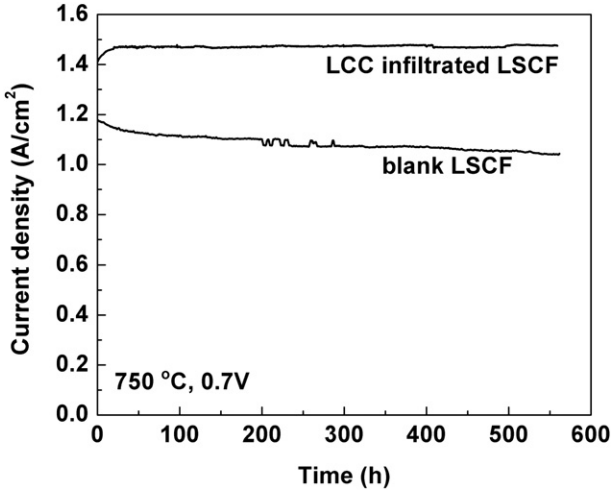

Fig. 7 – Long term stability of the anode-supported cells with and without LCC infiltration.

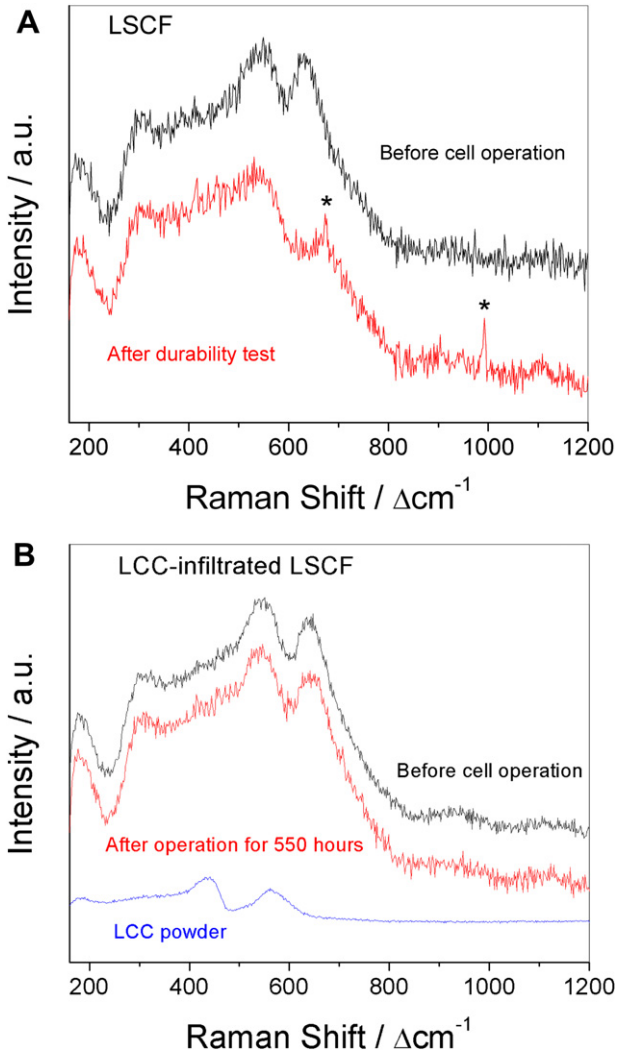

Fig. 8 – Typical Raman spectra collected from (A) LSCF and (B) LCC-infiltrated LSCF cathodes before/after durability tests, along with a spectrum collected from LCC powder.

degradation of the LSCF phase and the emergence of a new Raman active phase out of the original LSCF. The 675 cm^{-1} peak, in particular, might represent the A_{1g} mode of a Co_3O_4 phase that separated out of the LSCF [35]. These changes to the cathode material's phase composition are likely a major component of the performance degradation observed for the unmodified LSCF. On the other hand, as displayed in Fig. 8(B), spectra obtained from the LCC-infiltrated LSCF cathode both before and after long-term operation were largely similar; no new peaks nor notable changes in the peaks were observed after operation. As for evidence of the presence of LCC itself, one may note that the low loading amount of the nano-particles likely approaches the lower sensitivity limits of Raman spectroscopy. However, evidence could be seen in a small sloped shoulder centered at 435 cm^{-1} in the spectra for the LCC-infiltrated sample corresponding with a broad peak in the spectrum collected from LCC powder, which is also shown in Fig. 8(B). The spectra for the un-infiltrated LSCF are slightly less sloped in the same spot. In addition, a relatively higher peak intensity for 546 cm^{-1} versus the un-infiltrated LSCF spectra can be observed, corresponding with the other peak in the LCC powder spectrum. Although these spectral differences were subtle, the stabilizing effect of the LCC on the cathode was quite clear when comparing the sets of spectra in Fig. 8(A) and (B).

3.4. *Mechanism of enhancement*

It should be mentioned that improved performance has been demonstrated for SDC [19], YDC [36] and GDC [16] infiltration into LSCF. The improved performance resulted from the high ionic conductivity of the doped ceria, which significantly reduces electrode resistance for the oxygen migration/diffusion process [16,36]. However, compared to the aforementioned SDC and GDC, the conductivity of LCC was very low. Shown in Fig. 9 are the Arrhenius plots of the conductivities of SDC and LCC obtained in air. It was obvious that the conductivity of LCC was about one order of magnitude lower than that of SDC. The low conductivity of LCC might be the reason for the low performance when LCC infiltrant with higher concentration was loaded on LSCF cathode (shown in Fig. 4).

In order to better understand the catalytic contribution of LCC on LSCF surface, the functionality of LCC and SDC were also compared using symmetric cells. Fig. 10 compares the interfacial polarization resistance of the LSCF-LCC composite cathode with LSCF-SDC composite cathode and pure LSCF cathode. Clearly, the LSCF-SDC composite displayed much lower electrode polarization resistance than pure LSCF. At 750 °C, for example, the polarization resistance for LSCF-SDC was only 0.041 Ω cm^2, compared to 0.068 Ω cm^2 for the pure LSCF cathode. It is reported that the electro-catalytic activity of cathode can be significantly improved by adding oxygen ion conducting phases such as GDC or SDC to LSCF [2]. However, opposite behavior was observed when mixed the LCSF with LCC. The Rp was 0.15 Ω cm^2 at 750 °C for the LSCF-LCC composite cathode, about 2 times higher than that of pure LSCF. The low performance of the LSCF-LCC composite cathode indeed indicated that the LCC is not a good ionic conductor for enhancing the electro-catalytic properties of LSCF. However, when a thin coating or nano-particles of LCC

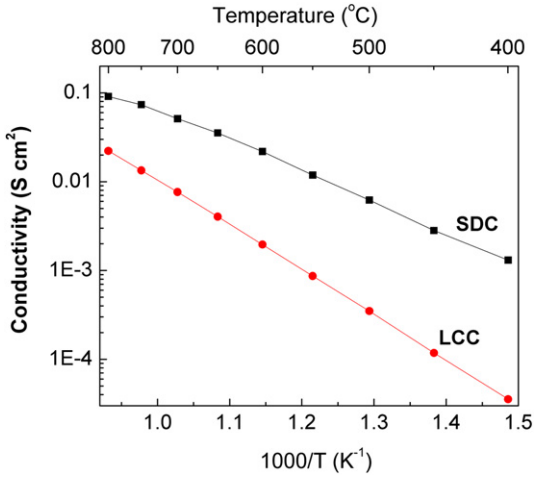

Fig. 9 – Ionic conductivities of LCC and SDC as measured from 800° to 400 °C in air.

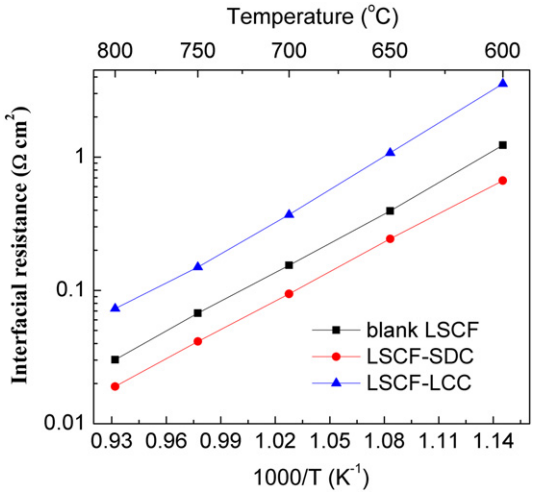

Fig. 10 – A comparison of the electrode polarization resistance of LSCF-SDC and LSCF-LCC composite cathode with pure LSCF cathode studied symmetric cells.

is applied via infiltration, a significant enhancement of the LSCF performance is achieved, which might result from the enhanced catalytic activity toward O_2 reduction on the surface. In other words, the LCC shows high surface kinetic toward O_2 reduction, but the total performance is limited by the low diffusion kinetics in the bulk.

It is should be noted that infiltration method demonstrated in the present work is different from that of being widely employed in fabricating SOFC composite electrodes: infiltration of an electronic conducting phase into an ionic conducting backbone [37–39] or infiltration of an ionic conducting phase into an electronic conducting backbone [40–45], where the infiltration steps should be repeated several times to form a connected network and provides a pathway for charge transfer (electronic for ionic). Generally, high loading weight ratio (~40–50 wt%) is required to achieve high electrode performance in those infiltration process. Compared to the conventional infiltration process, however, this new approach is simple and can be readily incorporated in the commercial available cells to enhance the performance and stability at low cost.

4. Conclusion

The present study demonstrated that both performance and stability of LSCF cathode can be enhanced by surface modification with an LCC catalyst coating, leading to ~18% improvement in peak power density and stable operation (without observable degradation) for over 550 h. It was found that nanoscale discrete LCC particles on the LSCF cathode can increase the active sites and enhance surface activity for oxygen reduction reaction on the LSCF surface. The cathode enhancement technique reported here only requires a simple infiltration process and post treatment, which can be easily incorporated into the current commercial cells to improve the performance and reliability at low cost. In order to further understand the intrinsic catalytic properties of LCC, more details of the electrochemical behavior under different cathodic bias and different PO_2 should be studied in the future. In addition, other techniques, such as electrical conductivity relaxation (ECR) techniques or oxygen-isotope exchange and depth profiling (IEDP) measurements, are needed to investigate surface exchange kinetics behavior of LCC.

Acknowledgments

This material is based upon work supported by the Department of Energy, National Energy Technology Laboratory, under Award Number DE-NT0006557 and by the Heterogeneous Functional Materials (HeteroFoaM) Center, an Energy Frontier Research Center funded by the U.S. Department of Energy, Office of Science, Office of Basic Energy Sciences under Award Number DE-SC0001061. Partial support of the WCU program at UNIST, South Korea, is also acknowledged.

REFERENCES

[1] Jiang SP. A comparison of O_2 reduction reactions on porous (La, Sr)MnO_3 and (La, Sr)(Co, Fe)O_3 electrodes. Solid State Ionics 2002;146(1–2):1–22.
[2] Murray EP, Sever MJ, Barnett SA. Electrochemical performance of (La, Sr)(Co, Fe)O_3–(Ce, Gd)O_3 composite cathodes. Solid State Ionics 2002;148(1–2):27–34.
[3] Yang L, Liu Z, Wang SZ, Choi YM, Zuo CD, Liu ML. A mixed proton, oxygen ion, and electron conducting cathode for SOFCs based on oxide proton conductors. J Power Sources 2010;195(2):471–4.
[4] Simner SP, Anderson MD, Engelhard MH, Stevenson JW. Degradation mechanisms of La–Sr–Co–Fe–O_3SOFC cathodes. Electrochem Solid-State Lett 2006;9(10): A478–81.
[5] Kim JY, Sprenkle VL, Canfield NL, Meinhardt KD, Chick LA. Effects of chrome contamination on the performance of $La_{0.6}Sr_{0.4}Co_{0.2}Fe_{0.8}O_3$ cathode used in solid oxide fuel cells. J Electrochem Soc 2006;153(5):A880–6.
[6] Benson SJ, Waller D, Kilner JA. Degradation of $La_{0.6}Sr_{0.4}Co_{0.2}Fe_{0.8}O_3$ in carbon dioxide and water atmospheres. J Electrochem Soc 1999;146(4):1305–9.
[7] Lane JA, Benson SJ, Waller D, Kilner JA. Oxygen transport in $La_{0.6}Sr_{0.4}Co_{0.2}Fe_{0.8}O_{3-\delta}$. Solid State Ionics 1999;121(1–4): 201–8.
[8] Lee JW, Liu Z, Yang L, Abernathy H, Choi SH, Kim HE, et al. Preparation of dense and uniform $La_{0.6}Sr_{0.4}Co_{0.2}Fe_{0.8}O_{3-\delta}$ (LSCF) films for fundamental studies of SOFC cathodes. J Power Sources 2009;190(2):307–10.
[9] Lynch ME, Yang L, Qin WT, Choi JJ, Liu MF, Blinn K, et al. Enhancement of $La_{0.6}Sr_{0.4}Co_{0.2}Fe_{0.8}O_{3-\delta}$ durability and surface electrocatalytic activity by $La_{0.85}Sr_{0.15}MnO_{3-\delta}$ investigated using a new test electrode platform. Energy Environ Sci 2011;4(6):2249.
[10] Hwang HJ, Ji-Woong MB, Seunghun LA, Lee EA. Electrochemical performance of LSCF-based composite cathodes for intermediate temperature SOFCs. J Power Sources 2005;145(2):243–8.
[11] Suzuki T, Jasinski P, Anderson HU, Dogan F. Role of composite cathodes in single chamber SOFC. J Electrochem Soc 2004;151(10):A1678–82.

[12] Muranaka M, Sasaki K, Suzuki A, Terai T. LSCF-Ag Cermet cathode for intermediate temperature solid oxide fuel cells. J Electrochem Soc 2009;156(6):B743–7.
[13] Zhang JD, Ji Y, Gao HB, He TM, Liu J. Composite cathode $La_{0.6}Sr_{0.4}Co_{0.2}Fe_{0.8}O_3$–$Sm_{0.1}Ce_{0.9}O_{1.95}$–Ag for intermediate-temperature solid oxide fuel cells. J Alloys Compd 2005; 395(1–2):322–5.
[14] Sahibzada M, Benson SJ, Rudkin RA, Kilner JA. Pd-promoted $La_{0.6}Sr_{0.4}Co_{0.2}Fe_{0.8}O_3$ cathodes. Solid State Ionics 1998;115: 285–90.
[15] Sakito Y, Hirano A, Imanishi N, Takeda Y, Yamamoto O, Liu Y. Silver infiltrated $La_{0.6}Sr_{0.4}Co_{0.2}Fe_{0.8}O_3$ cathodes for intermediate temperature solid oxide fuel cells. J Power Sources 2008;182(2):476–81.
[16] Chen J, Liang FL, Chi B, Pu J, Jiang SP, Jian L. Palladium and ceria infiltrated $La_{0.8}Sr_{0.2}Co_{0.5}Fe_{0.5}O_{3-\delta}$ cathodes of solid oxide fuel cells. J Power Sources 2009;194(1):275–80.
[17] Liu ML, Liu Z, Liu MF, Nie LF, Mebane DS, Wilson DS, Surdoval W. "Solid oxide fuel cells having porous cathodes infiltrated with oxygen-reducing catalysts", US Patent Application No. 12/837,757.
[18] Lou XY, Wang SZ, Liu Z, Yang L, Liu ML. Improving $La_{0.6}Sr_{0.4}Co_{0.2}Fe_{0.8}O_{3-\delta}$ cathode performance by infiltration of a $Sm_{0.5}Sr_{0.5}CoO_{3-\delta}$ coating. Solid State Ionics 2009; 180(23–25):1285–9.
[19] Nie LF, Liu MF, Zhang YJ, Liu ML. $La_{0.6}Sr_{0.4}Co_{0.2}Fe_{0.8}O_{3-\delta}$ cathodes infiltrated with samarium-doped cerium oxide for solid oxide fuel cells. J Power Sources 2010;195(15):4704–8.
[20] Steele BCH, Middleton PH, Rudkin RA. Material Science Aspects of Sofc technology with Special Reference to anode Development. Solid State Ionics 1990;40-1:388–93.
[21] Miki T, Ogawa T, Haneda M, Kakuta N, Ueno A, Tateishi S, et al. Enhanced oxygen storage Capacity of cerium oxides in $CeO_2/La_2O_3/Al_2O_3$ Containing precious Metals. J Phys Chem 1990;94(16):6464–7.
[22] Gao JF, Liu XQ, Peng DK, Meng GY. Electrochemical behavior of $La_{0.6}Sr_{0.4}Co_{0.2}Fe_{0.8}O_{3-\delta}$ (Ln = Ce, Gd, Sm, Dy) materials used as cathode of IT-SOFC. Catal Today 2003;82(1–4):207–11.
[23] Yokokawa H, Sakai N, Horita T, Yamaji K, Brito ME, Kishimoto H. Thermodynamic and kinetic considerations on degradations in solid oxide fuel cell cathodes. J Alloys Compd 2008;452(1):41–7.
[24] Nie LF, Liu Z, Liu MF, Yang L, Zhang YJ, Liu ML. Enhanced performance of $La_{0.6}Sr_{0.4}Co_{0.2}Fe_{0.8}O_{3-\delta}$ (LSCF) cathodes with Graded microstructure fabricated by tape casting. J Electrochemical Sci Technol 2010;1(1):50–6.
[25] Liu MF, Peng RR, Dong DH, Gao JF, Liu XQ, Meng GY. Direct liquid methanol-fueled solid oxide fuel cell. J Power Sources 2008;185(1):188–92.
[26] Ding D, Liu B, Zhu Z, Zhou S, Xia C. High reactive $Ce_{0.8}Sm_{0.2}O_{1.9}$ powders via a carbonate co-precipitation method as electrolytes for low-temperature solid oxide fuel cells. Solid State Ionics 2008;179(21–26):896–9.
[27] Liu MF, Dong DH, Peng RR, Gao JF, Diwu J, Liu XQ, et al. YSZ-based SOFC with modified electrode/electrolyte interfaces for operating at temperature lower than 650 degrees C. J Power Sources 2008;180(1):215–20.
[28] Liu MF, Gao JF, Dong DH, Liu XQ, Meng GY. Comparative study on the performance of tubular and button cells with YSZ membrane fabricated by a refined particle suspension coating technique. Int J Hydrogen Energy 2010;35(19): 10489–94.
[29] Wang WS, Gross MD, Vohs JM, Gorte RJ. The stability of LSF-YSZ electrodes prepared by infiltration. J Electrochem Soc 2007;154(5):B439–45.
[30] Baumann FS, Fleig J, Konuma M, Starke U, Habermeier HU, Maier J. Strong performance improvement of $La_{0.6}Sr_{0.4}Co_{0.2}Fe_{0.8}O_{3-\delta}$ SOFC cathodes by electrochemical activation. J Electrochem Soc 2005;152(10):A2074–9.
[31] Lin Y, Zhan Z, Liu J, Barnett S. Direct operation of solid oxide fuel cells with methane fuel. Solid State Ionics 2005; 176(23–24):1827–35.
[32] Tietz F, Haanappel VAC, Mai A, Mertens J, Stover D. Performance of LSCF cathodes in cell tests. J Power Sources 2006;156(1):20–2.
[33] Varshney D, Kumar A, Verma K. Effect of A site and B site doping on structural, thermal, and dielectric properties of BiFeO(3) ceramics. J Alloys Compd 2011;509(33):8421–6.
[34] Tai LW, Nasrallah MM, Anderson HU, Sparlin DM, Sehlin SR. Structure and electrical-properties of $La_{1-x}Sr_xCo_{1-y}Fe_yO_3$ .2. The system $La_{1-x}SrxCo_{0.2}Fe_{0.8}O_3$. Solid State Ionics 1995; 76(3–4):273–83.
[35] Hadjiev VG, Iliev MN, Vergilov IV. The Raman-spectra of Co3o4. J Phys C Solid State Phys 1988;21(7):L199–201.
[36] Sholklapper TZ, Kurokawa H, Jacobson CP, Visco SJ, De Jonghe LC. Nanostructured solid oxide fuel cell electrodes. Nano Lett 2007;7(7):2136–41.
[37] Huang Y, Vohs JM, Gorte RJ. SOFC cathodes prepared by infiltration with various LSM precursors. Electrochem Solid-State Lett 2006;9(5):A237–40.
[38] Sholklapper TZ, Lu C, Jacobson CP, Visco SJ, De Jonghe LC. LSM-infiltrated solid oxide fuel cell cathodes. Electrochem Solid-State Lett 2006;9(8):A376–8.
[39] Shah M, Barnett SA. Solid oxide fuel cell cathodes by infiltration of La0.6Sr0.4Co0.2Fe0.8O3-(delta) into Gd-Doped Ceria. Solid State Ionics 2008;179(35–36):2059–64.
[40] Xu XY, Jiang ZY, Fan X, Xia CR. LSM-SDC electrodes fabricated with an ion-impregnating process for SOFCs with doped ceria electrolytes. Solid State Ionics 2006;177(19–25): 2113–7.
[41] Jiang SP, Leng YJ, Chan SH, Khor KA. Development of (La, Sr) MnO3-based cathodes for intermediate temperature solid oxide fuel cells. Electrochem Solid-State Lett 2003;6(4): A67–70.
[42] Jiang SP, Wang W. Fabrication and performance of GDC-impregnated (La, Sr)MnO3 cathodes for intermediate temperature solid oxide fuel cells. J Electrochem Soc 2005; 152(7):A1398–408.
[43] Jiang SP, Wang W. Novel structured mixed ionic and electronic conducting cathodes of solid oxide fuel cells. Solid State Ionics 2005;176(15–16):1351–7.
[44] Zhang L, Zhao F, Peng RR, Xia CR. Effect of firing temperature on the performance of LSM-SDC cathodes prepared with an ion-impregnation method. Solid State Ionics 2008; 179(27–32):1553–6.
[45] Tian RF, Fan J, Liu Y, Xia CR. Low-temperature solid oxide fuel cells with La1-xSrxMnO3 as the cathodes. J Power Sources 2008;185(2):1247–51.